Urban Ecosyst (2018) 21:183–195
DOI 10.1007/s11252-017-0693-y

Evaluating the effectiveness of urban trees to mitigate storm water runoff via transpiration and stemflow

Sybil G. Gotsch[1] · **Danel Draguljić**[2] · **Christopher J. Williams**[3]

Published online: 1 August 2017

Abstract Many cities in the Eastern United States are working to increase urban tree cover due to the hydrological services that trees provide, including the interception, storage and transpiration of water that would otherwise enter sewer systems. Despite the understanding that trees benefit urban ecosystems, there have been few studies that address the underlying physiology of different urban trees with regard to their capacity to take up water, particularly following rain events. We monitored the sap flow of nine species of trees in urban parks and linked sap flow to local microclimate. In addition, we measured throughfall, stemflow and crown architecture. Interspecific variation in sap flow was significant as were differences in time lags (i.e. difference in time between the increase of solar radiation versus sap flow) across species of large but not small trees. Interestingly the most important microclimatic drivers of sap flow were different in large versus small trees. Lastly, we found that trees with a large branch angle routed more rainwater to stemflow. In this study we found strong evidence that variation in urban tree physiology can impact important hydrological services that will influence the effectiveness of different trees as tools to manage stormwater runoff.

✉ Sybil G. Gotsch
sybil.gotsch@fandm.edu

[1] Department of Biology, Franklin and Marshall College, PO Box 3003, Lancaster, PA 17603, USA

[2] Department of Mathematics, Franklin and Marshall College, PO Box 3003, Lancaster, PA 17603, USA

[3] Department of Earth and Environment, Franklin and Marshall College, PO Box 3003, Lancaster, PA 17603, USA

Keywords Branch angle · Ecohydrology · Microclimatic drivers · Sap flow · Stemflow · Throughfall

Introduction

Over the last 55 years there has been a 70% increase in the amount of rain that falls during heavy precipitation events in the Northeastern United States (Walsh et al. 2014). During this period, there has also been an increase in the frequency of large rainfall events in this region (Walsh et al. 2014). Whereas projected changes in climate are likely to cause drought in many parts of the world, the Northeastern Region of the United States is projected to receive continued increases in precipitation and the frequency of large rainfall events (Horton et al. 2014). An increase in the frequency of large storms would in turn lead to increases in small and large scale flooding, erosion and pollution of watersheds.

While the projected changes in precipitation patterns will affect rural, suburban and urban ecosystems, there are unique challenges in urban ecosystems due to the high percentage of impermeable ground cover in the built environment. Green infrastructure (e.g. green roofs, rain gardens and tree plantings) can greatly mitigate storm water run-off in urban areas by capturing, storing, evaporating and transpiring water that would otherwise enter sewer systems (Xiao 1998; Bolund and Hunhammar 1999; Xiao and McPherson 2016; Palla et al. 2010). Such management strategies present a solution to mitigate storm water runoff, and provide additional ecosystem benefits including air purification and a reduction of the heat island effect (Beckett et al. 1998; Jorgensen and Gobster 2010; Jenerette et al. 2011).

Although an increase in any type of vegetative cover can provide health and ecosystem benefits to the urban environment, an increase in the urban tree canopy can be particularly

valuable given the high leaf area, water storage capacity, transpiration rates, and carbon sequestration capacity of trees. In 2001, the urban tree canopy on average in the U.S. was estimated at 27% and despite many documented benefits of the urban forest on ecosystem processes and human health, the percent tree cover in a number of large cities in the U.S. has declined (Beckett et al. 1998; Nowak et al. 2001; Jorgensen and Gobster 2010; Jenerette et al. 2011; Nowak and Greenfield 2012). Tree planting campaigns are currently underway in a number of cities including the large metropolitan areas of New York City (milliontreesnyc.org), Philadelphia (plantonemillion.org), and Washington, D.C. (http://www.stateforesters.org/state/district-columbia) with goals of total tree canopy cover ranging from 35 to 40%. Globally, it has been estimated that approximately 50% of the water that falls on vegetated surfaces is recycled (Chahine 1992). Attaining these urban planting goals would result in a substantive proportion of the water that falls on the landscape being recycled locally rather than being diverted into sewer systems and lost from the ecosystem.

While increasing the urban canopy with any species of tree would likely provide a number of ecosystem benefits, it is important to consider the ecophysiological traits specific to different species. In cities in the arid Southwest of the U.S., researchers have evaluated street trees to determine the extent to which the urban forest directly competes with human populations for water (Bijoor et al. 2012). In a recent study, researchers investigated the canopy surface storage of common landscaping species and found almost 4-fold variation across the 13 study species (Holder and Gibbes 2017). In these water-limited environments, the goal is to maximize ecosystem functions that benefit the urban ecosystem while simultaneously minimizing water use.

In areas of the country such as the Northeastern U.S. where precipitation is abundant and expected to increase, the most successful street trees will be those that intercept water during a rainfall event and then transpire the greatest amount of water immediately following that event. Interception and stemflow have been shown to be affected by traits including crown leaf area, branch angle and bark roughness (Schooling and Carlyle-Moses 2015). While crown interception can slow the path of water into the sewer system, the greatest benefits of urban trees may lie in their ability to take up water and release it back into the atmosphere via transpiration. Common Eastern trees such as Sycamores, Maples and Ashes have been shown to move large volumes of water in Eastern Forests, but their ability to initiate transpiration quickly following a storm has not been studied (Bowden and Bauerle 2008; Herbst et al. 2008; Pataki et al. 2011). In this study we measured rates of water uptake, stem flow and throughfall of large and small individuals of common trees in the city of Lancaster, Pennsylvania, USA to evaluate which species may be most successful at mitigating storm water run-off. Specifically, we asked the following questions:

1. Which species and size class increase water uptake most quickly following a precipitation event?
2. Which species experience the greatest total sap flow following a precipitation event?
3. Do the microclimatic drivers of sap flow differ for large and small trees?
4. Which species maximize stemflow and can branch angle predict stemflow?

Methods

Study site and species

This study took place in three locations within the city limits of Lancaster Pennsylvania (40° 2′59.64″ N, 76° 16′27.1194″ W). The average annual temperature is 11.5 °C, the average annual high temperature is 17.1 °C and the average low temperature is 6.0 °C. The average annual precipitation is 1087 mm and the average annual snowfall is 46 cm (http://www.usclimatedata.com).

We studied common street tree species from May to October of 2015. Measurements were made on large (50.8–91.4 cm DBH) trees in two urban parks (Long's Park and Reservoir Park) that are 3 miles apart (Table 1). In Reservoir Park, we evaluated two individuals of *Platanus occidentalis* and one individual of *Acer saccarum* while in Long's park we evaluated two individuals of both *Fraxinus americana* and *Acer platanoides*. Individuals chosen were in healthy condition, within 10 m of one another, and climbable. We also evaluated seven small trees in an urban street tree demonstration plot located in Buchanan Park (Table 1). All the small trees had a DBH between 5 and 10 cm. While the majority of these species are being promoted as street trees, *Fraxinus americana* is no longer being promoted due to the widespread threat of the *Agrilus planipennis* (Emerald Ash Borer) and the cost associated with maintaining the health of this species. We measured sap flow on all study trees throughout the growing season. On the small trees we also measured branch angle, stem flow and throughfall.

Sap flow

Two sap flow methods were employed on the different sized trees. Large trees were outfitted with internal heat ratio probes (Burgess et al. 2001) while small trees were outfitted with external heat ratio sap flow sensors (Clearwater et al. 2009). Both types of probes were constructed in the Gotsch lab at Franklin and Marshall College.

The internal sensors consist of a heater probe that is flanked by thermocouple probes (each containing three thermocouples), while the external sensors contain a small resistor

Table 1 General information for the species evaluated in this study

Scientific name	Common Name	Native Region	Tree Type	Appx. Max height
Acer ginnala	Amur maple	Asia	Ornamental	10 m
Acer griseum	Paperbark maple	Central China	Ornamental	10 m
Acer platanoides	Norway maple	Europe & W. Asia	Large	30 m
Acer rubrum	Red maple	United States	Med-Large	25 m
Acer saccarum	Sugar maple	United States	Large Tree	30 m
Fraxinus americana	White ash	United States	Med-Large	25 m
Ginko biloba	Gold ginko	China	Large	35 m
Parrottia sp.	Parrottia	Asia	Ornamental	10 m
Platanus occidentalis	American sycamore	United States	Large	35 m
Taxodium distichum	Bald cyprus	United States	Large	35 m
Zelkova serrata	Green vase	Asia	Large	30 m

(heater) flanked by two small thermocouples and these three components are all installed in a common silicone backing (Gotsch et al. 2014, 2015). Every 10 min, a pulse of heat was sent to the heater, and the ratio of the increase in temperature was measured at two points equidistant downstream and upstream from the heat source. Two sensor sets were installed on either side of the main trunk in each of the large trees. These sensors were installed approximately 7 m off the ground to ensure the safety of the equipment. The sap flow stations on large trees were installed and maintained using arborist climbing techniques. The sensors were connected to a common multiplexer and datalogger (CR1000 and AM16/32; Campbell Scientific Inc., Logan, UT, USA) with 10 m long cables. A 12 V battery powered the sap flow station. The external sap flow systems were installed on secondary branches and were all connected to a common datalogger on the ground. Since this equipment was more vulnerable than the stations that were installed in the mid-canopy, we limited our measurements of small trees to the test plot that was close to the Franklin and Marshall College campus.

Heat pulse velocity, V_h (cm/h), was calculated using the equation

$$V_h = \frac{k}{x} \ln\left(\frac{\delta T_1}{\delta T_2}\right) \quad (1)$$

where x represents the distance between the heater and the thermocouple, δT_1 and δT_2 are the downstream and upstream temperature changes (°C), and k represents the thermal diffusivity constant estimated from

$$k = \frac{x^2}{4t_m} \mathrm{cm^2 s^{-1}} \quad (2)$$

where t_m is the time between the heat pulse and the maximum temperature measured x distance above and below the heater (Clearwater et al. 2009). This allowed for the determination of sap flow velocity, V_s, from

$$V_s = \frac{V_h \rho_b (c_w + m_c c_s)}{\rho_s c_s} \quad (3)$$

where ρ_b is the stem density, c_W is the specific heat capacity of the wood matrix (1200 J kg^{-1} $°C^{-1}$ at 20 °C), c_S is the specific heat capacity of water (4182 J kg^{-1} $°C^{-1}$ at 20 °C), m_c is the water content of the xylem and ρ_s is the density of water (Burgess et al. 2001).

Volumetric sap flow (L/h) was determined by multiplying average sap velocity by the sap wood area. Sapwood area for each tree was evaluated at the end of the experiment by removing a core of wood, whose length was the radius of the stem, with an increment borer. This sample was then viewed directly to detect differences between the sapwood and heartwood. If no clear differences were seen between the sapwood and heartwood, the sample was soaked in ethanol and viewed with a light table and stereoscope to detect the distinct tissue layers (Githiomi and Dougal 2012). For the small trees, the entire branch was considered sapwood.

Sap flow stations were installed in April 2015 and operated through October 2015. Data for the internal sensors were processed to correct for wounding following Burgess et al. (2001).

Each internal thermocouple needle was equipped with three thermocouples at depths of 0.5, 1.7 and 3 cm from the base of the needle. Prior to installation, the bark was removed with a small knife to ensure installation directly into the xylem. The three probes were installed using a metal drill bit guide to ensure that they were installed perpendicular to the trunk and equidistant from one another. The distance between the heater probe and the top and bottom thermocouple needles was 0.6 cm for the internal probes and 0.5 cm for the external probes (Burgess et al. 2001; Clearwater et al. 2009). Prior to installation, internal sensors were coated with petroleum jelly to improve heat conduction. Molding clay and aluminum foil

were placed over the exterior portion of the sensors to minimize natural temperature gradients due to direct or indirect radiation. The external sensors were placed directly on the stems and were wrapped in parafilm and aluminum foil to ensure a close connection between the sensor and the branch and to minimize temperature gradients due to solar radiation.

At the end of the study, all sensor sets were individually calibrated. For the internal sensors this was achieved by drilling a hole above and below the sensor sets to sever the xylem, thereby stopping sap flow. For the external sensors, the entire branch was cut above and below the sensor. Sap flow systems then collected data for three additional days (to ensure that we captured at least one sunny day). Once it was clear that the systems were reading zero flow (based on flat lining of the curve, not the absolute value), the average flow rate for a 24 h flat-line period was used as the 'true zero' rate. The data for each sensor set were adjusted accordingly.

Weather station

A Vaisala WXT520 weather transmitter was used to measure air temperature, relative humidity, barometric pressure and rainfall duration and intensity. The sensors are located 2.5 m above a vegetated surface in a nature preserve (40° 3′12.56″ N, 76° 20′23.78″ W) located 1 km from the Long's Park site and 4.5 km from Reservoir Park. Sensor readings were collected every 5 min and stored as 15 min averages on a NexSens 3100-iSIC datalogger. Cumulative hourly rainfall was calculated using NexSens iChart software (v.6.18.002). Hourly average solar radiation data were acquired from the Pennsylvania Department of Environmental Protection Ambient Air Monitoring Data Report database (http://www.ahs.dep.pa.gov/aq_apps/aadata). These data are collected at a continuously operated air quality monitoring station (EPA-AQS site code: 42-071-0007; 40° 2′48.63″ N, 76° 17′00.51″ W) located in close proximity to Reservoir Park (0.9 km) and near the Long's Park (5.2 km) site.

Stemflow, throughfall and canopy architecture

Stemflow, a component of the hydrological cycle that refers to the amount of rainwater that runs parallel along the main stem, is an important factor to delay the entry of water into a sewer system. Stem flow facilitates rainwater being absorbed by soil in the tree planting area rather than falling directly on impermeable surfaces. Stemflow gauges were constructed by affixing half of a length of flexible tubing around the small trees using epoxy. The tubing was long enough to wrap around the tree stem a minimum of three times. The end of the tubing was placed into a plastic bottle for collection. After every rain event the volume of water was measured in a graduated cylinder and the bottles were emptied.

Throughfall refers to the water that drips through the canopy during a rain event. We measured this parameter to detect which species maximized the stemflow to throughfall ratio since throughfall is likely to drip onto impervious surfaces while stem flow is likely to enter into tree wells and the soil. Throughfall gauges were constructed using an outer cylinder of PVC that was fit with a funnel (473 ml capacity) and collection bottle. The diameter of the funnel was 140 mm, which was slightly larger than the diameter of the PVC. The collection bottle was connected to the end of the funnel with a piece of hose. Stakes were fixed to the bottom of the gauge to sustain the gauges in an upright position. Three gauges were placed under each of the small trees. The gauges were adjusted with a level to ensure a vertical position. The total throughfall under every tree was quantified after every rain event.

Both branch angle and total leaf area were quantified on each of the small trees (Harbor Freight, Digital Angle Gauge). The branch angle was measured halfway along the branch on three branches on each of the trees. To quantify total leaf area, all of the leaves were taken from one secondary branch and the average leaf area was determined by measuring the total area of the leaf sample with a leaf area meter (Licor 3100C) and dividing that number by the total number of leaves. The total number of leaves was then counted on each of the small trees and this value was multiplied by the average leaf area.

Analyses

All analyses were carried out separately for the small and large trees. The analyzed data consisted of hourly averages for each tree. Since we were interested in the tree's sap flow following a nightly rainfall event (i.e. the rainfall that occurred when solar radiation was 0 W/m^2), we focused on all dry periods (i.e. when rainfall was 0 mm) that followed periods of the nightly rainfall and that lasted until at most the following dawn. We were able to identify 15 such periods. Due to the technical issues, we were not able to collect the data for small trees on September 11th, which resulted in one less period for the small trees.

For each tree and for each period, we calculated M, the maximum sap flow (L/h), F the total sap flow (L), S, the maximum rate of change in sap flow as a function of time for any 4 h consecutive time period (L/h^2), and D, the hourly difference between the start of the 4 h period associated with S and the 4 h period associated with maximum increase in solar radiation (hours). A summary of these metrics can be found in Table 2. The most effective candidate to mitigate the storm water run-off would have maximum M, F, and S with the minimum D. Evaluation of M and S were limited to days following a rain event when there was sunshine at least through the morning and noon period when sap flow is expected to increase most quickly and achieve maximum rates. Evaluation of F was limited to days following a rain event when all daylight hours were cloud and rain free. We analyzed

Table 2 Summary information for the calculated sap flow metrics for the large and small study trees

Metric	Definition	Abbreviation	Units
Max flow rate	Maximum sap flow rate in a 24 h period	*M*	L/h
Daily flow	Total daily sap flow in a 24 h period	*F*	L
Slope	Maximum rate of change in sap flow as a function of time for any 4 h consecutive time period	*S*	L/h2
Time Lag	Hourly difference between the start of the 4 h period associated with *S* and the 4 h period associated with maximum increase in solar radiation	*D*	hours

the relationship between *M*, *F*, and *S*. If these three variables showed high correlation, we planned to analyze only *S* since *S* requires fewer hours of sunlight to evaluate the pattern of water use. If these variables were not strongly related, we planned to run separate analyses with each parameter. The analysis of *D* was carried out separately from other variables.

To compare the sap flow between different species a random effect ANOVA model with an effect for species was

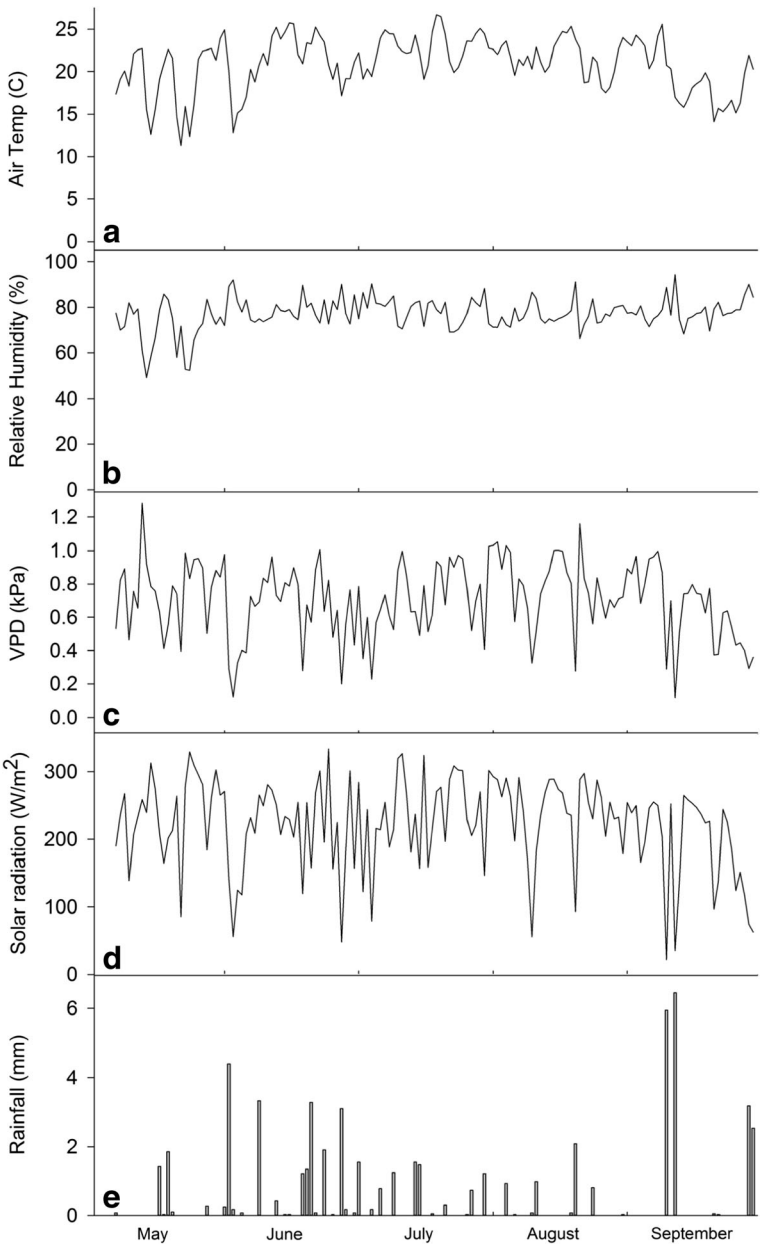

Fig. 1 Microclimate in Lancaster, PA from May to September of 2015. Average daily air temperature (**a**), relative humidity (**b**), vapor pressure deficit (**c**), and solar radiation (**d**) during the study period. Daily total precipitation is shown in panel (**e**)

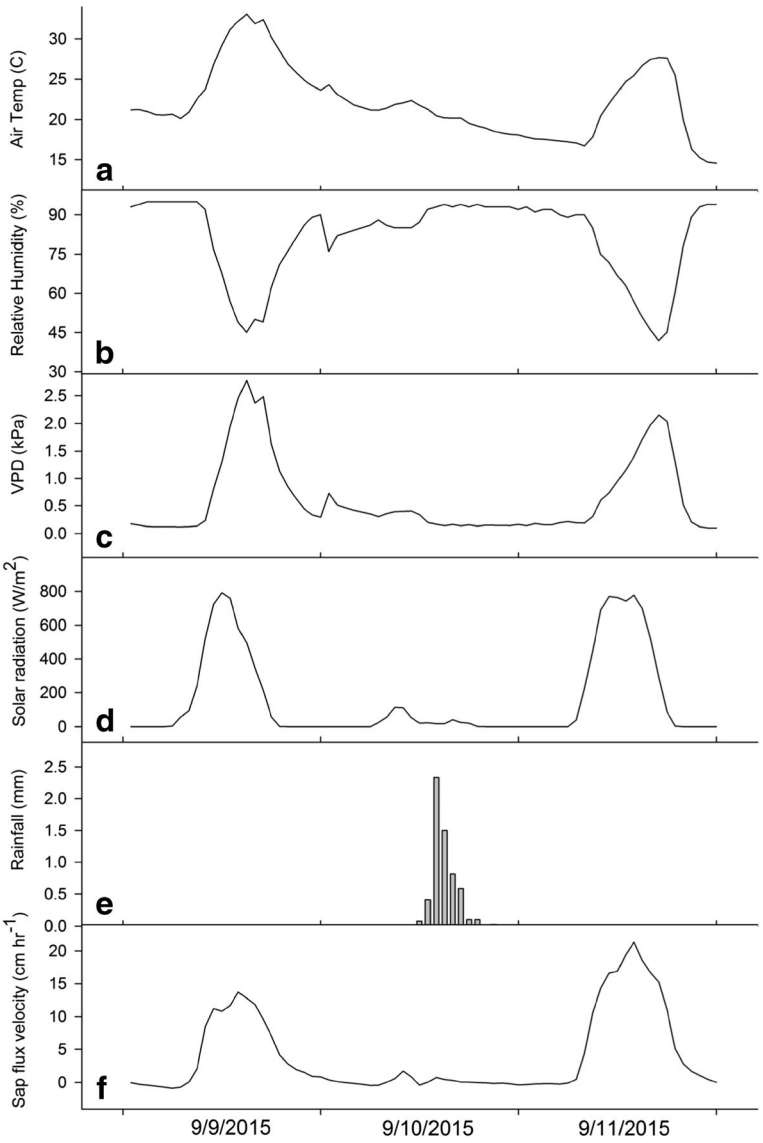

Fig. 2 Hourly microclimate and sap flow for three representative daily periods during the present study. Average hourly temperature (**a**), relative humidity (**b**), vapor pressure deficit (**c**), solar radiation (**d**), and the total hourly precipitation (**e**) from 9/9/2015 to 9/10/2015. Hourly sap flow during the same period is shown in panel (**f**)

used. If this model found a significant difference between species, all pairwise comparisons with Tukey's adjustment were carried out. For large trees, one tree of *Acer sacarrum* was measured while two trees were measured of the other species. For our analyses on large trees, we combined the plants within species with the realization that, if there was a significant nested effect of plant within species, our results were conservative. To analyze variable D, we used a Kruskal-Wallis rank sum test. If this test found significant differences between species, we tested the pairwise differences via a Wilcoxon test with a Bonferroni multiplicity adjustment.

To determine the environmental drivers of sap flow we fitted a hierarchical linear (mixed) model. The initial model contained the random effect of species and plant nested within species (for large trees only), and the fixed effects of solar radiation, temperature, and relative humidity. We considered vapor pressure deficit as an explanatory variable, but decided to exclude it from our analyses after inspecting solar radiation, temperature, relative humidity, and vapor pressure deficit for multicolinearity. The fixed effects included three main effects, three quadratic effects, and three two-way interaction effects. The higher order interactions were assumed to be negligible. All parameters were estimated via maximum likelihood. To eliminate the effects deemed insignificant and to construct a parsimonious model we performed a backward selection. The backward selection was performed by fitting the model and eliminating the fixed term with the highest p-value. An exception to this rule was made to accommodate the *effect hierarchy* in our model, i.e. if an interaction effect was in the model then so were the two main effects that comprised that interaction. If one of the main effects, which was involved in a two-way interaction still in the model, was identified for elimination, then this main effect was held in the model and the term with

next highest *p*-value was removed. The same exception was applied to the main effects whose quadratic effect was significant in the model.

To assess the adequacy of the term elimination, we used the Likelihood-ratio test (LRT) to compare the fit of the model with the fixed term associated with the highest *p*-value and the model without this term. If the LRT failed to reject the hypothesis that the likelihood of observing the data under each model is not statistically significant at $\alpha = 0.05$, the elimination was accepted and the process was repeated. If the LRT rejected at $\alpha = 0.05$, the elimination was rejected, the procedure was stopped, and the final model was identified.

Except the nonparametric Kruskal-Wallis and Wilcoxon tests, all models were fitted to log-transformed data values. The logarithmic (base 10) transformation improved the assumptions of normality and homogeneity of variance. Relationships between branch angle and leaf area with the ratio of throughfall to stem flow were analyzed using a linear regression. All data analyses were completed using the statistical program *R*.

Results

Microclimate

We collected sap flow and microclimate data from April through October. The first and last months of sap flow in this data series were significantly lower than the late spring and summer months and were therefore excluded from our analyses. From May through September, the average daily air temperature fluctuated from 12 to 25 °C and the average over the entire period was 19.2 °C (Fig. 1a). The relative humidity also fluctuated but values were generally between 70 and 80%. The average was 77.2% and there were only a few days when the humidity was below 50% (Fig. 1b). The calculated average VPD throughout the study was 0.65 kPa. The range of VPD during the study period was from 0.1 to 1.3 kPa (Fig. 1c). The daily average solar radiation ranged from 20 to 325 W/m^2 throughout the study period and the average solar radiation was 207.3 W/m^2 (Fig. 1d). A total of 613.1 mm of rain fell during the study period (Fig. 1e) and there were 48 distinct rain events (rain events occurring over 2 d were counted twice). While there were many small events that only provided 0.01–0.5 mm of rain, there were also seven events that provided over 2.5 mm of rain.

Sap flow

Sap flow was very responsive to meteorological conditions during this study. During periods of high solar radiation, VPD and air temperature, and low relative humidity, sap flow generally increased (Fig. 2). During periods of precipitation, low VPD and high relative humidity, sap flow rates decreased or ceased entirely (Fig. 2).

Patterns of sap flow across trees (research questions 1 and 2)

Figures 3 and 4 illustrate diurnal courses for sap flow in large and small trees and the comparison of slopes for the increase in sap flow in comparison to the increase in solar radiation. Large trees

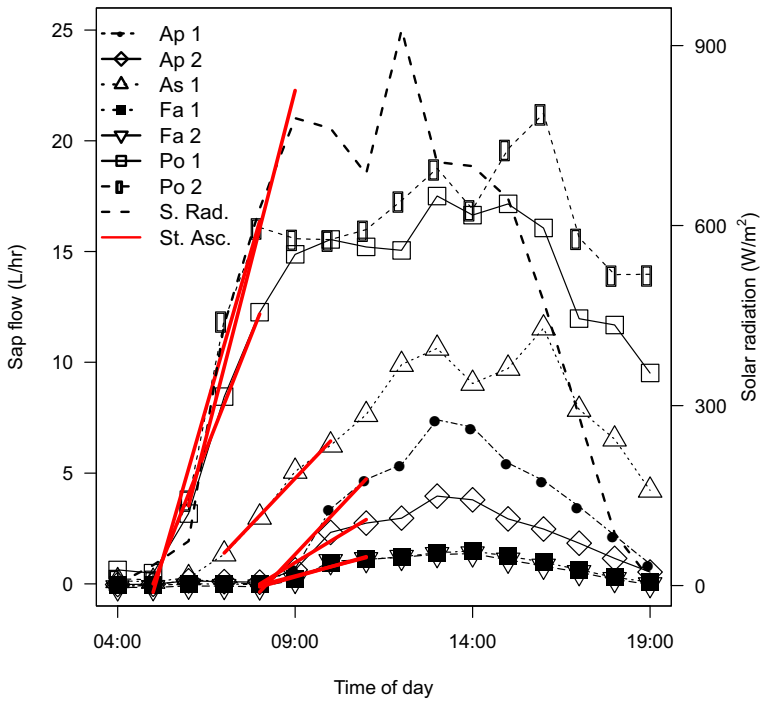

Fig. 3 Representative diurnal sap flow for the large trees evaluated in this study from 9/9/2015 to 9/10/2015. Abbreviations in the legend represent the genus (*first letter*) followed by the species name (*second letter*) of the study trees. Full names can be found in Table 1. The *fitted lines* indicate points used to calculate the slope of the maximum daily increase in sap flow as well as the slope of the increase in solar radiation in the morning or following a rain event (*S. Rad.* and *St. Asc.*, respectively). These slope lines were used to calculate the delay in sap flow following a rain event. The legend indicates each of the species with the first letter of the genus followed by the first letter of the species (see Table 1)

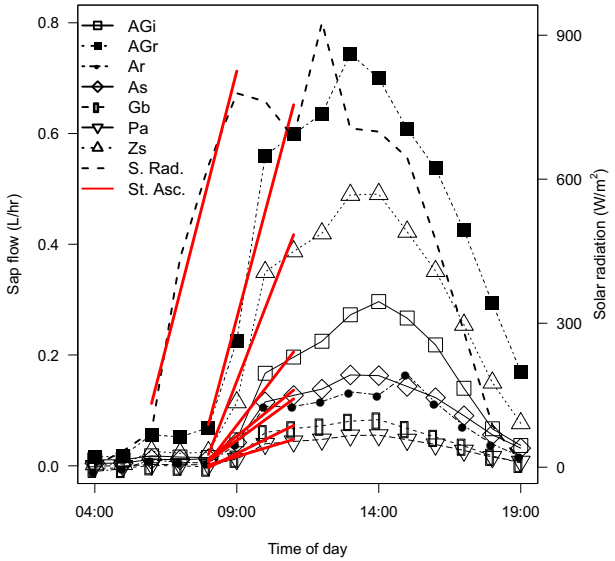

Fig. 4 Representative diurnal sap flow for the small trees evaluated in this study. Abbreviations in the legend represent the genus (*first letter*) followed by the species name (*second letter*) of the study trees. Full names can be found in Table 1. The *fitted lines* indicate points used to calculate the slope of the maximum daily increase in sap flow as well as the slope of the increase in solar radiation in the morning or following a rain event (*S Rad.* and *St. Asc.*, respectively). These slope lines were used to calculate the delay in sap flow following a rain event. The legend indicates each of the species with the first letter of the genus followed by the first letter of the species (see Table 1)

varied greatly in *M* and these values ranged from less than 5 L/h to over 20 L/H. *Platanus occidentalis* generally had the highest *M* while *Fraxinus americana* generally had the lowest (Fig. 3). For small trees, patterns of sap flow were similar to large trees but *F* and *M* were an order of magnitude lower (Fig. 4). The highest sap flow in the small trees was generally expressed by *Acer griseum* while the lowest values were often expressed by *Parrotia sp.* and *Ginko biloba* (Fig. 4).

Across the study period, we found a significant linear relationship between *S* and *F* (Fig. 5a), *S* and *M* (Fig. 5b), and *F* and *M* (Fig. 5c, Table 2 for explanation of calculated metrics). In all three cases, the correlation coefficient was above 0.94. Since *S, M,* and *F* were highly correlated, the remainder of our analyses employed only *S*.

We examined *S,* the maximum rate of change in sap flow, across the study period for large and small trees and found that there were significant differences in these values for both tree sizes (small trees: $F_{6,\ 94} = 54.84$, $P < 0.0001$; large trees: $F_{3,\ 101} = 144.14$, $P < 0.0001$, Figs. 6 and 7). All pairwise comparisons indicated significant differences between the large trees (largest Tukey adjusted $P = 0.0210$ between *Acer platanoides* and *Acer saccarum*; all other *P*-values were less than 0.0001). For example, Fig. 6 shows that *Platanus occidentalis* had the greatest *S* on average (and therefore maximum flow rates and total flow) throughout the study. *Fraxinus americana* consistently had the lowest *S* values of the large trees throughout the study (Fig. 6).

The two species of small trees that exhibited the highest *S* were *Zelkova serrata* and *Acer griseum* and the rates of increase of these trees were not significantly different from one another (Fig. 7). *Acer ginnala* and *Acer saccarum* exhibited relatively moderate values of *S* and these two trees were also not significantly different from one another (Fig. 7).

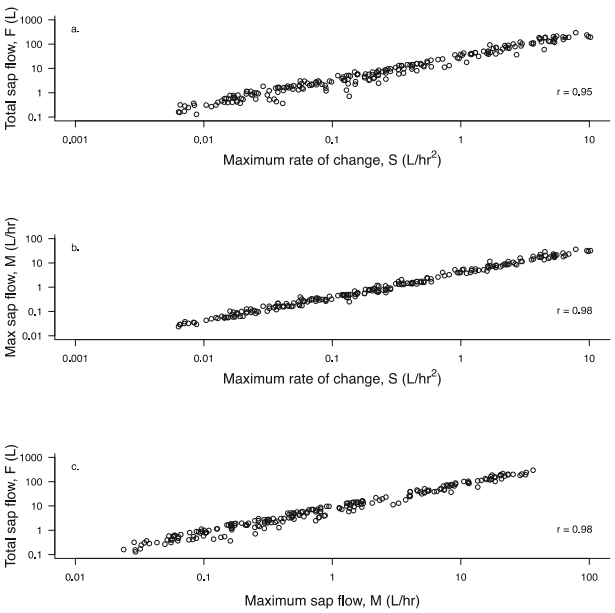

Fig. 5 The relationship between, (**a**) the maximum slope of the diurnal sap flow course (max slope) and the total daily volumetric sap flow (L), (**b**) the max slope and the maximum sap flow rate (L/h) and, (**c**) the maximum sap flow (L) and the total daily volumetric flow for all trees throughout the study period

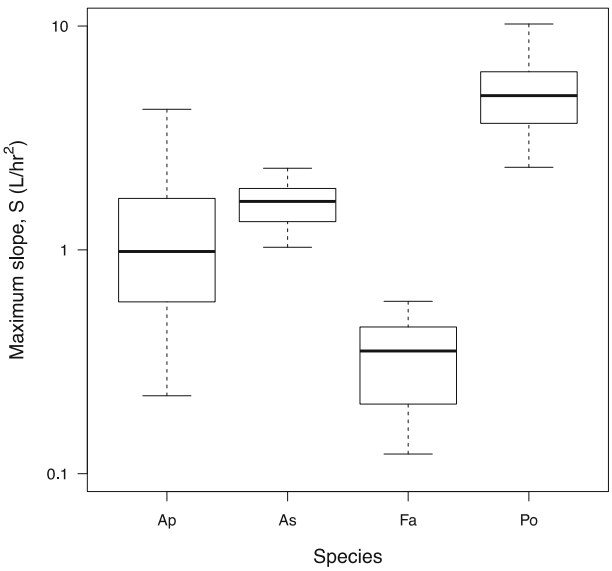

Fig. 6 The maximum slope of sap flow for the four large tree species throughout the study period. The x-axis indicates each of the species with the first letter of the genus followed by the first letter of the species (see Table 1). There was a significant species effect ($F_{3,\ 101} = 144.14$, $P < 0.0001$). All pairwise comparisons with Tukey's adjustment were significant

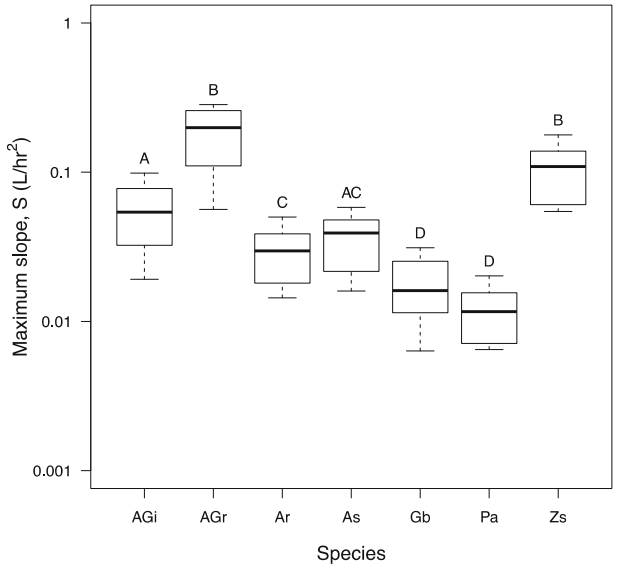

Fig. 7 The maximum slope of sap flow for the seven small tree species throughout the study period. The x-axis indicates each of the species with the first letter of the genus followed by the first letter of the species (see Table 1). A random effect ANOVA model revealed a significant effect of species for the maximum slope ($F_{6, 94} = 54.84$, $P < 0.0001$). The species labeled with different letters were significantly different from each other ($P \leq 0.05$) in Tukey's pairwise comparison tests

Furthermore, there was no significant difference in *S* of the two small individuals of the *Acer* species (Fig. 7). *Ginkgo biloba* and *Parrotia sp.* consistently exhibited the lowest *S* of the small trees (Fig. 7).

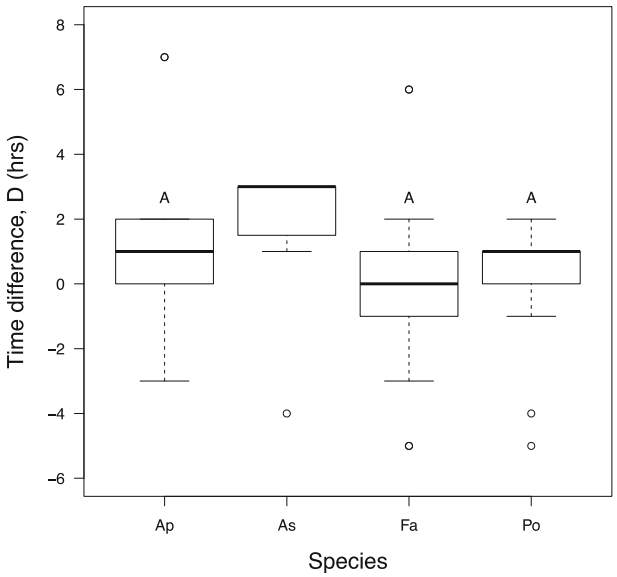

Fig. 8 The hourly difference (*D*) between the start of the 4-h period associated with maximum increase in sap flow, *S* and the start of the 4 h period associated with maximum increase in solar radiation for large trees. The x-axis indicates each of the species with the first letter of the genus followed by the first letter of the species (see Table 1). The Kruskal-Wallis test revealed a significant species effect (KW = 16.03 with 3 df and $P = 0.0010$). The species labeled with the same letter were not significantly different from each other in pairwise comparisons with Bonferroni's adjustment

The effect of species was significant in the analysis of the time difference (i.e. sap flow lag, variable *D*) for large trees (KW = 16.03 with 3 df and $P = 0.0010$, Fig. 8). There was no significant difference between *D* for *Acer platanoides, Fraxinus americana,* and *Platanus occidentalis* (medians were equal to 1, 0, and 1 h, respectively). *Acer saccarum* (median = 3 h) exhibited significantly different *D* from all other species. There was no difference in *D* among small trees (KW = 1.12 with 6 df and $P = 0.9807$). The median *D* ranged from 0 to 1 h and the ranges within species were large (Fig. 9).

Microclimatic drivers of sap flow in large and small trees (research question 3)

In the first hierarchical (mixed) linear model analysis, we examined the effect that variation in microclimate had on sap flow in the small trees. There were $n = 98$ observations in this analysis. The full model contained 9 fixed effects (main and quadratic terms for temperature, relative humidity and solar radiation as well as the two-way interaction terms). Scaled estimates of the final model obtained by performing the backward selection were calculated to allow for comparison of the relative effect of the different terms in the model. The linear and quadratic terms for relative humidity and the linear term for solar radiation were all significant in the final model ($P < 0.0001$) but relative humidity had the largest effect on the sap flow of small trees. As the relative humidity increased, the sap flow of small trees decreased. See Table 3 for the summary of the results.

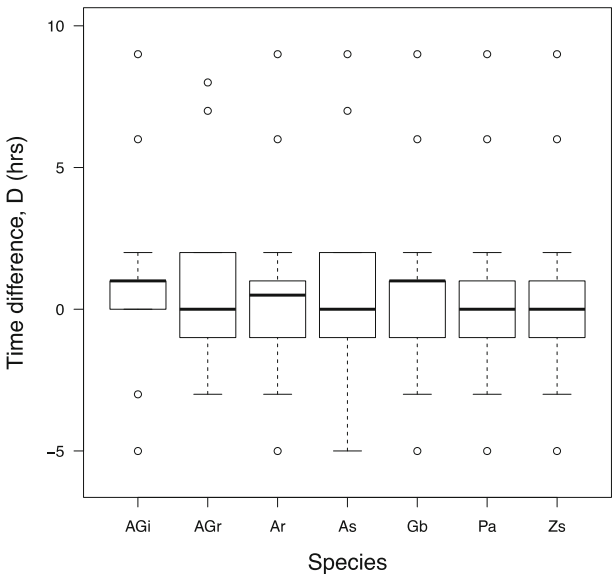

Fig. 9 The hourly difference (*D*) between the start of the 4-h period associated with maximum increase in sap flow, *S* and the start of the 4 h period associated with maximum increase in solar radiation for small trees. The x-axis indicates each of the species with the first letter of the genus followed by the first letter of the species (see Table 1). A Kruskal-Wallis rank sum test indicated that there was no effect of species on the time difference for the small trees

Table 3 A summary of fixed effects in the final model examining the effect of microclimate on sap flow for small trees

Effect	Estimate	Scaled Estimate	*t* value	*p*-value
Solar radiation	0.0013	0.0361	5.96	<0.0001
Relative humidity	−0.1054	0.2906	−5.33	<0.0001
Relative humidity^2	0.0008	0.0313	5.68	<0.0001

The *Effect* column lists the effects that were significant in the final model. The *Estimate* column shows the estimated values of the regression coefficients on the original scale, while the *Scaled Estimate* column lists the estimated values of the regression coefficients when each explanatory variable was scaled to have a standard deviation of 1 prior to analysis. This metric was calculated to examine the relative effect of the different drivers on transpiration. The last two columns correspond to the *t* and two-sided *p*-values for each of the effects respectively

In the second hierarchical (mixed) linear model analysis, we examined the effect that variation in microclimate had on sap flow in the large trees. There were $n = 100$ observations in this analysis. The full model contained 9 fixed effects (main and quadratic terms for temperature, relative humidity and solar radiation as well as the two-way interaction terms). Relative humidity and solar radiation were both significant in the final model ($P < 0.0001$) but solar radiation had the largest effect on the sap flow of large trees. As the solar radiation increased, so did the sap flow of large trees. See Table 4 for the summary of the results.

Table 5 and Fig. 10 show the simple linear regression analyses results and plots between observed and predicted sap flow values. The linear regression analyses indicated good fits between the observed and predicted values. Both slope and intercept estimates were near 1 and 0, respectively, and the r^2 values were 0.86 and 0.84 for small and large trees, respectively.

Crown architecture and patterns of external flow (research question 4)

Branch angle varied greatly across the species. The shallowest branch angle in the study was exhibited by *Taxodium distichum* (15.6 °C SE = 1.2°) and the sharpest was exhibited by *Zelkova serrata* (66.2 °C SE +/− 3.3). We found a negative relationship between the branch angle and the ratio of throughfall to stemflow (Fig. 11). The species that exhibited higher branch angles also facilitated a greater proportion of water flow down the main stem of the tree. The total estimated leaf area also varied greatly across the trees. Of the small trees, *Zelkova serrata* had the greatest crown leaf area (35.5 m^2) and *Parrottia sp*. had the smallest crown area (4 m^2). We found no significant relationship between total crown leaf area and the ratio of throughfall to stemflow (data not shown).

Table 4 A summary of fixed effects in the final model examining the effect of microclimate on sap flow for large trees

Effect	Estimate	Scaled Estimate	*t* value	*p*-value
Solar radiation	0.0008	0.1563	4.45	<0.0001
Relative humidity	0.0189	0.1699	4.86	<0.0001

The *Effect* column lists the effects that were significant in the final model. The *Estimate* column shows the estimated values of the regression coefficients on the original scale, while the *Scaled Estimate* column lists the estimated values of the regression coefficients when each explanatory variable was scaled to have a standard deviation of 1 prior to analysis. This metric was calculated to examine the relative effect of the different drivers on transpiration. The last two columns correspond to the *t* and two-sided *p*-values for each of the effects respectively

Table 5 A summary of simple linear regression analyses carried out to assess how well the models fit the data

Analysis	Coefficient	Estimate	*t* value	*p*-value	R^2
Small trees	β_0	0.0173	0.29	0.7750	0.86
	β_1	1.0122	24.73	<0.0001	
Large trees	β_0	−0.0006	−0.03	0.9780	0.84
	β_1	1.0075	23.45	<0.0001	

The response variable was the $\log_{10}$ of the observed sap flow values and the explanatory variable was the ln of the predicted sap flow values. See Fig. 10 for a graphical display of these analyses. The first model analyzes the effect of microclimatic drivers on small trees and the second model analyzes the effect of microclimatic drivers on large trees

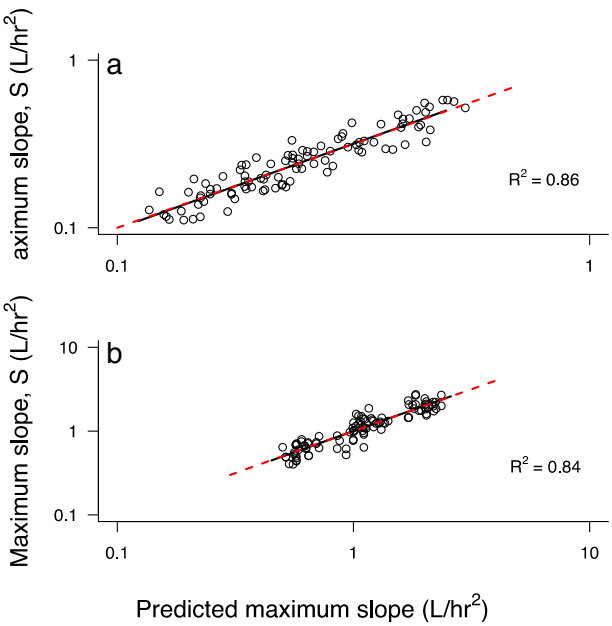

Fig. 10 Performance of the models created to evaluate the effect of microclimatic drivers on sap flow for small (**a**) and large (**b**) trees. The response variable was the log of the observed sap flow values and the explanatory variable was the log of the predicted sap flow values. A summary of the analyses can be found in Table 4. The *line* represents the simple linear regression line. The dashed line represents a reference line whose intercept and slope are 0 and 1, respectively

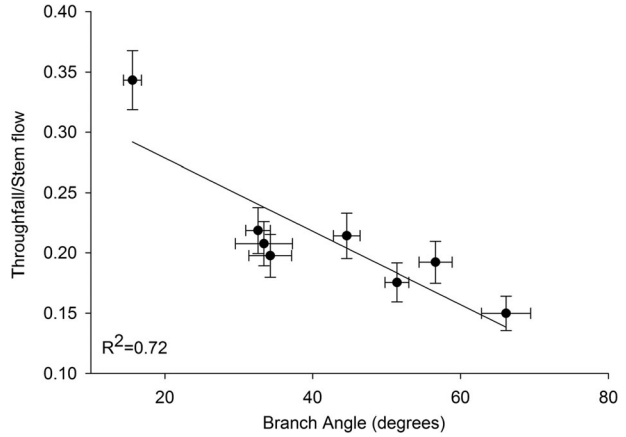

Fig. 11 The relationship between branch angle and the ratio between throughfall (mm) and stemflow (mm) for the eight small trees included in this study. The best fit linear regression line is shown and the R^2 corresponding to this analysis is in the *lower left* of the panel. The *error bars* represent the standard error of the mean for throughfall/stemflow and the branch angle

Discussion

Our results indicate that variation in tree form and function can greatly affect the degree to which trees in urban ecosystems can impact stormwater mitigation (research questions 1 and 2). *S* was highest overall in *Platanus occidentalis* and lowest in *Fraxinus americana*. The slopes were an order of magnitude greater in *Platanus occidentalis* which corresponded with a 4–5 fold increase in the maximum sap flow rates and total daily sap flow on average (see Figs. 3 and 6). Declines in *Fraxinus sp*. have become widespread in the Eastern United States due to the exotic pest, *Agrilus planipennis* (emerald ash borer) which tunnels underneath the bark of the host and destroys the radial cambium (Herms and McCullough 2014). While the emerald ash borer has been found on trees in Lancaster PA, there were no signs of tree damage or the presence of the borer in our study trees. We also found significant variation in *S* of the small trees (Figs. 4 and 7). *Acer griseum* and *Zelkova serrata* consistently exhibited between a 5–7 fold increase in *M* (L/h) and *F* (L) when compared with *Parrotia sp*. and *Ginkgo biloba*. Interestingly these differences were not due to tree type. *Parrotia sp.* and *Acer griseum* are both small ornamental trees while *Zelkova serrata* and *Ginkgo biloba* can grow to a mature height of 30 m.

To ameliorate the effects of stormwater run-off, a better understanding of the responsiveness of sap flow patterns following rain events is required. We found a significant difference in *D* in the large trees indicating the presence of a time lag in sap flow for some species (research question 1, Fig. 8). Despite having the lowest overall sap flow, *Fraxinus americana* exhibited no average lag between the initiation of sap flow and an increase in solar radiation meaning that this species responded quickly to increases in solar radiation following rain events. *Platanus occidentalis*, the species that exhibited the greatest sap flow, also did not exhibit a lag in sap flow following a rain event. Although both species were equally responsive in our study, given the overall rates of flow, *Platanus occidentalis* would confer a much greater benefit in stormwater mitigation. In contrast, *Acer rubrum*, exhibited an average time lag of 3 h. This species is one of the most widely naturally occurring species in Eastern North America and is also a common street tree in the region as well (Walters and Yawney 1990). While highly valued for its autumn color and its ability to thrive in a variety of conditions, *Acer rubrum* is slow to respond to rainfall and therefore maybe more well suited in urban areas where run-off is less problematic (Walters and Yawney 1990). In contrast with large trees, there was no significant difference in the initiation of sap flow following an increase in solar radiation in small trees (Fig. 9). Since there is sufficient root space in the park where these trees are planted, it is possible that a greater proportion of their roots are superficial which would enable a faster increase in sap flow following a rain event. Species-specific differences, such as those seen for the large trees, are likely to present themselves as these smaller individuals develop since there was a large difference in rates of sap flow and these species represent both small ornamental and medium to large trees at maturity.

We saw no indication of a reduction of the sap flow signal during dry periods in this study. We expected that a high water user such as *Platanus occidentalis* would have experienced drought suppression but we found no evidence of this for *Platanus* or any other species. The summer of 2015 was relatively wet which did not provide much of an opportunity to detect drought stress in our study trees. Despite climate projections calling for an increase in average annual rainfall, increases in dry periods are also projected which are likely to cause widespread mortality of some species (Hoffmann et al. 2011; Horton et al. 2014; Walsh et al. 2014). While *Platanus* maybe a suitable tree to inhabit urban areas for the mitigation of stormwater runoff, we suggest additional sap flow studies that include drier periods to determine drought tolerance of this species in the urban environment. Furthermore, all the trees in this study were located in urban parks. Despite being in an urban ecosystem, these trees experience less limitation than street trees, which have limited rooting area. Rates of transpiration are likely to be lower in street plantings where soil water availability is more limited. We suggest future work on street trees where individuals are more likely to experience drought stress, such as in confined tree wells.

We found that both large and small trees were very responsive to changes in microclimate, although the most important drivers differed across size classes and species (research question 3). Patterns of transpiration of small trees were primarily driven by variation in relative humidity while variation in solar radiation had the most important impact on sap flow of large trees. Since drought did not seem to have an important

impact on sap flow in the study, the drivers analysis can tell us how the study trees are influenced by variation in microclimate in the absence of water stress. The primary driver of sap flow in large trees was solar radiation. Regardless of other microclimatic parameters, an increase in solar radiation resulted in an increase in sap flow, which is likely coupled to rates of photosynthesis in these trees. Surprisingly, sap flow in the small trees was not influenced by solar radiation to the same extent. For small trees, the most important driver of sap flow was the relative humidity. Increases in the relative humidity lead to decreases in sap flow. While patterns of sap flow may often have a tight relationship with stomatal conductance and photosynthesis, in this case these parameters may be decoupled from one another. The small trees in this study were under 10 ft tall. At this height, the gravimetric potential in the leaves at the top of the tree would not have exceeded −0.01 MPa. Under well-watered and humid conditions in short trees, the gravimetric potential may have been overcome leading to a breakdown in the water potential gradient that causes vertical water movement in plants. If this were the case, the stomata might have been closed, but they could have also been open (i.e. photosynthesis taking place) and we would not have necessarily detected a change in whole-plant water flow.

Steep branch angles were related to a greater proportion of the total amount of intercepted water being delivered to the base of the tree via stemflow (research question 4, Fig. 11). In the urban environment it is important to consider the maximization of stemflow because during rain events, more of the rainfall will run into the tree planting area rather than dripping through the canopy onto impermeable surfaces. These findings support recent work that also found a positive relationship between branch angle and stemflow (Carlyle-Moses and Schooling 2015; Schooling and Carlyle-Moses 2015).

In this study we found great variation in maximum sap flow rates and significant variation in the time lags of large trees. Such differences are likely to be perpetuated through the urban forest community. Since it is not feasible to determine sap flow properties of all species, we suggest that future research efforts focus on unraveling relationships between patterns of canopy interception and sap flow with underlying tree and leaf traits. Studies addressing the physiology and ecohydrology of urban trees provide critical information for urban planners as they work to design urban forests that achieve desired ecosystem services. By linking physiological processes with leaf and canopy functional traits, we will move closer toward a cost–effective and efficient predictive physiology-based method to be utilized by urban planners and urban forest managers.

Acknowledgements The authors would like to thank the City of Lancaster (Department of Public Works, in particular Karl Greybill) and the Lancaster County Conservancy (Fritz Schroeder) for supporting this work. The authors would like to acknowledge SGG's students from her Ecophysiology Seminar Course: Rai Abdulhusein, Max Aleman, Rob King, Kate Leibow, Molly Lowell, Julia Rosenwald, Sucel Sanchez and Ryan Stull for help constructing stem flow and throughfall gauges and for help deploying sensors in Buchanan Park. We also acknowledge Lex Darby for his help with experimental installation, data collection and site maintenance. This work was funded by Franklin and Marshall College.

Author contributions SGG formulated the ideas resulting in the research. SGG and her students constructed and deployed the sensors. DD conducted statistical and modeling analyses and contributed text regarding those analyses. CW installed and maintained the weather station and contributed text regarding the meteorological measurements. SGG wrote the manuscript. All authors edited the manuscript.

References

Beckett KP, Freer-Smith PH, Taylor G (1998) Urban woodlands: their role in reducing the effects of particulate pollution. Environ Pollut 99(3):347–360

Bijoor NS, McCarthy HR, Zhang DC, Pataki DE (2012) Water sources of urban trees in the Los Angeles metropolitan area. Urban Ecosyst 15: 195–214

Bolund P, Hunhammar S (1999) Ecosystem services in urban areas. Ecol Econ 29:293–301

Bowden JD, Bauerle WL (2008) Measuring and modeling the variation in species-specific transpiration in temperate deciduous hardwoods. Tree Physiol 28:1675–1683

Burgess SSO, Adams M, Turner NC, Beverly CR, Ong CK, Khan AAH, Bleby TM (2001) An improved heat pulse method to measure low and reverse rates of sap flow in woody plants. Tree Physiol 21:589–598

Carlyle-Moses DE, Schooling JT (2015) Tree traits and meteorological factors influencing the initiation and rate of stemflow from isolated deciduous trees. Hydrol Process 29:4083–4099

Chahine MT (1992) The hydrological cycle and its influence on climate. Nature 359:373–380

Clearwater MJ, Luo Z, Mazzeo M, Dichio B (2009) An external heatpulse method for measurement of sap flow through fruit pedicels, leaf petioles and other small-diameter stems. Plant Cell Environ 32:1652–1663

Githiomi JK, Dougal E (2012) Analysis of heartwood –sapwood demarcation methods and variation of sapwood and heartwood within and between 15 year old plantation grown *Eucalyptus Regnans*. Int J Appl Sci Technol 2:8

Gotsch SG, Asbjornsen H, Weintraub AE, Holwerda F, Goldsmith GR, Dawson TE (2014) Foggy days and dry nights determine crown-level water balance in a seasonal tropical montane cloud forest. Plant Cell Environ 37(1):261–272

Gotsch SG, Nadkarni N, Darby A, Glunk A, Dix M, Davidson K, Dawson T (2015) Life in the treetops: ecophysiological strategies of canopy epiphytes in a tropical montane cloud forest. Ecol Monogr 85(3):393–412

Herbst M, Rosier PTW, Morecroft MD, Gowing DJ (2008) Comparative measurements of transpiration and canopy conductance in two mixed deciduous woodlands differing in structure and species composition. Tree Physiol 28:959–970

Herms DA, McCullough DG (2014) Emerald ash borer invasion of North America: history, biology, ecology, impact and management. Annu Rev Entomol 59:13–30

Hoffmann WA, Marchin R, Abit P, Lau OL (2011) Hydraulic failure and tree dieback are associated with high wood density in a temperate forest under extreme drought. Glob Chang Biol 8:2731–2742

Holder CD, Gibbes C (2017) Influence of leaf and canopy characteristics on rainfall interception and urban hydrology. Hydrol Sci J 62(2): 182–190. doi:10.1080/02626667.2016.1217414

Horton R, Yohe G, Easterling W, Kates R, Ruth M, Sussman E, Whelchel A, Wolfe D, Lipschultz F (2014) Ch. 16: Northeast. In: Melillo JM, Richmond T (TC), Yohe GW (eds) Climate change impacts in the United States: the third national climate assessment. U.S. Global Change Research Program

Jenerette GD, Harlan SL, Stefanov WL, Martin CA (2011) Ecosystem services and urban heat riskscape moderation: water, green spaces, and social inequality in Phoenix, USA. Ecol Appl 21:2637–2651

Jorgensen A, Gobster PH (2010) Shades of green: measuring the ecology of urban green space in the context of human health and well-being. Nature & Culture 5:338–363

Nowak DJ, Greenfield EJ (2012) Tree and impervious cover change in U.S. cities. Urban For Urban Green 11(1):21–30

Nowak DJ, Noble MH, Sisinni SM, Dwyer JF (2001) Assessing the US urban forest resources. J For 99(3):37–42

Palla A, Gnecco I, Lanza LG (2010) Hydrologic restoration in the urban environment using green roofs. Water 2:140–154

Pataki DE, McCarthy HR, Litvak E, Pincetl S (2011) Transpiration of urban forests in the Los Angeles metropolitan area. Ecol Appl 21:661–677

Schooling JT, Carlyle-Moses DE (2015) The influence of rainfall depth class and deciduous tree traits on stemflow production in an urban park. Urban Ecosyst 18:1261–1284

Walsh J, Wuebbles D, Hayhoe K, Kossin J, Kunkel K, Stephens G, Thorne P, Vose R, Wehner M, Willis J, Anderson D, Doney S, Feely R, Hennon P, Kharin V, Knutson T, Landerer F, Lenton T, Kennedy J, Somerville R (2014) Ch. 2: our changing climate. In: Melillo JM, Terese (T.C.) Richmond, Yohe GW (eds) Climate change impacts in the United States: the third national climate assessment. U.S. Global Change Research Program, 19–67. doi:10.7930/J0KW5CXT

Walters RS, Yawney HW (1990) *Acer rubrum* L. red maple. In: Burns RM, Honkala BH (eds) Technical coordinators. Silvics of North America. Vol. 2. Hardwoods. Agric. Handb. 654. U.S. Department of Agriculture, Forest Service, Washington, DC, pp 60–69

Xiao Q (1998) Rainfall interception by Sacramento's urban forest. J Arboric 24:4

Xiao QF, McPherson EG (2016) Surface water storage capacity of twenty tree species in Davis, California. J Environ Qual 45:188–198